System Level Model of Damping Effects for Highly Perforated Torsional Microstructures

Gabriele Schrag, Robert Sattler and Gerhard Wachutka
Institute for Physics of Electrotechnology, Munich University of Technology, Germany
Arcisstr. 21, 80290 Munich, Germany
E-mail: sattler@tep.ei.tum.de

Abstract: We propose a mixed-level simulation scheme for squeeze film damping (SQFD) effects in micro-devices, which makes it possible to include damping effects in system-level models of entire microsystems in a natural, physical-based, and flexible way. Our approach allows also for complex geometries, large deflections and coupling to other energy and signal domains. Applying the methodology to torsional structures yields results which are in excellent agreement with accurate FEM simulations based on the 3D Navier-Stokes equations, thus demonstrating the practicality and quality of our approach. For device geometries with densely distributed perforations we propose a further order reduction by merging adjacent holes in one equivalent network element; in this way we are able to simulate highly perforated structures at affordable computational expense. The predictive simulation of an industrial microrelay featuring 3000 perforations validated by experimental analysis, illustrates the power of our methodology.

I. INTRODUCTION

Electrostatic torsional actuator are commonly used to act as basic elements in tiltable micromirrors [1] or micro-switches [2]. Especially the dynamic behavior of such microdevices is of particular interest, since micromirrors and microswitches have to be optimized with respect to the time needed to reach the maximum deflection and to return to the initial position. Here, as an inherent problem it turns out, that the dynamics is strongly affected by viscous air damping effects. In order to include these effects in device models there are basically three strategies: Either, heuristic damping terms are introduced in the model as empirical fit parameters [1,3], however, these have no specific physical meaning and do not scale with the design dimensions. Or analytical [4] approximations are used; but these are applicable to simple geometries and small deflections only. Alternatively, damping effects can be accurately analyzed on a physical basis by solving the highly complicated Navier Stokes equation (NSE). However, this approach easily becomes prohibitive because of the excessive computational expense which is required, if couplings between different physical energy domains have to be included and/or if complex device geometries have to be analyzed.

II. MODELING

We avoid this dilemma by following a new mixed-level approach, which makes it possible to reduce the model complexity by incorporating the damping effects on a physical basis and without perceptible loss of accuracy. Besides it offers high flexibility with respect to variations of the device geometry and coupling between different energy and signal domains. The basic ideas of our approach have been reported in [5]. The model is based on the Reynolds equation, a simplified version of the NSE, which assumes laminar gas flow and that gravitation, inertia forces and vertical pressure variations in the air gap can be neglected; these assumptions are valid under most of the operating conditions typical of MEMS devices.

$$\mathrm{div}\,\vec{j} = -\dot{\rho} + source \qquad (1)$$

$$\vec{j} = -\frac{\rho h^3}{12\eta}\nabla p \qquad (2)$$

$$\mathrm{div}\,\frac{\rho h^3}{12\eta}\nabla p = h\dot{\rho} - \rho\dot{h} \qquad (3)$$

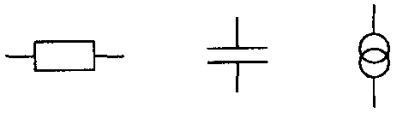

Fig. 1: Components of the finite network.

Finite Network Model:
Analogous to and compatible with the description of electric circuits as Kirchhoffian network, we use a Finite Network discretization of the Reynolds equation. In the terminology of Kirchhoffian Network variables, we consider the fluidic massflow as generalized flux

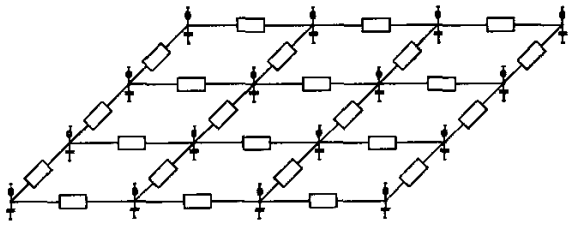

Fig. 2: Netlist of the finite network.

("through" variable), which is driven by the gradient of pressure acting as generalized force ("across" variable). Like other physical quantities obeying a conservation law and a potential–driven linear transport law, the Reynolds equation (3) results from combining the general mass conservation equation (1) with the constitutive current relation (2) for the gas flow.

In a finite network the respective potential is discretized, in such a way that all terms in the continuity equation can be represented by symbols known from electric networks (Fig. 1). The network elements are described in a hardware description language such as VHDL–AMS or Verilog–A. The netlist reflects the geometry of the structure. For a rectangular plate the netlist is visualized in Fig. 2. The generation of the netlist has been automated by a self written utility which converts the node and element information of a finite element mesh into a netlist. So you can benefit from a professional mesh tool to generate a proper finite network.

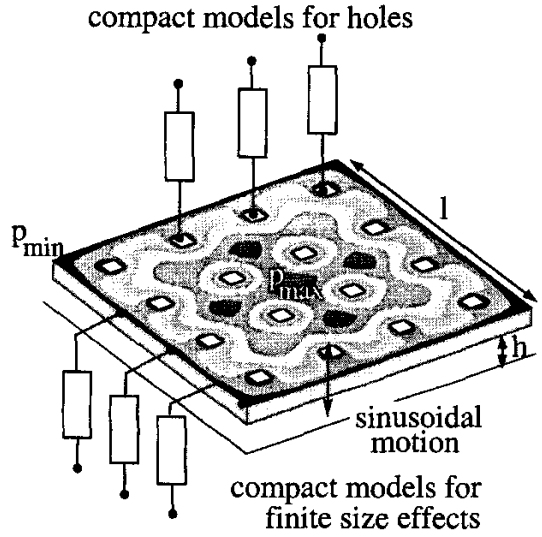

Fig. 3: Corrections for finite and perforated structures.

Corrections for the Reynolds equation:

The finite network can solve the Reynolds equation, but the latter is only valid if the lateral dimensions of the structure are much larger than the thickness of the fluid film. In order to account for boundary effects, corrections have to be added along the edges of the structure and at the edge holes. To this end, special

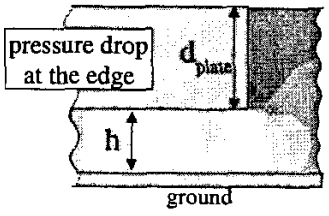

$$R_f = \frac{12\eta}{\rho h^3}\frac{l_{eff}}{l_{edge}} \quad (4)$$

$$l_{eff} = \lambda_f \cdot h$$

Fig. 4: Pressure drop at the edge.

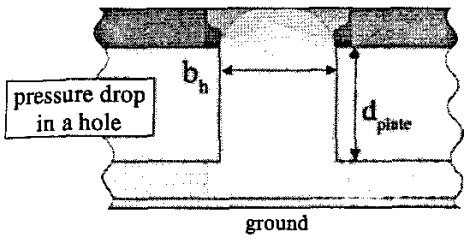

Fig. 5: Pressure drop in a hole.

network elements are included as compact models, which are equivalent to fluidic resistances that control the airflow between the cavity under the plate and the environment (Fig. 3).

The fluidic resistance (4) acting along the edges of the structure can be derived in analogy to the electric resistance. It is proportional to the inverse of the material constant in the Reynolds equation (2), to an effective length and to the inverse of the length of the edge of the structure.

The fluidic resistance that accounts for the pressure drop at the location of a hole is composed of two parts:

$$\frac{1}{2}\rho V v^2 = pV \quad (5)$$

$$Q_a = \rho v A = b_h^2 \sqrt{2\rho p}\cdot\lambda_a$$

The flow through an aperture, which can be derived by equating the fluidic kinetic energy to the hydrostatic energy (5).

$$Q_{ch} = \frac{\rho\, b_h^4\, p}{32\cdot\lambda_{ch}\,\eta\, d_{plate}} \quad (6)$$

The flow through a square shaped channel, which can be derived from the law of Hagen–Poiseuille (6).

Both models include a fitparameter λ, which has to be calibrated by FEM simulations.

III. RESULTS

We applied our method to torsional structures and investigated tiltable perforated and non–perforated plates.

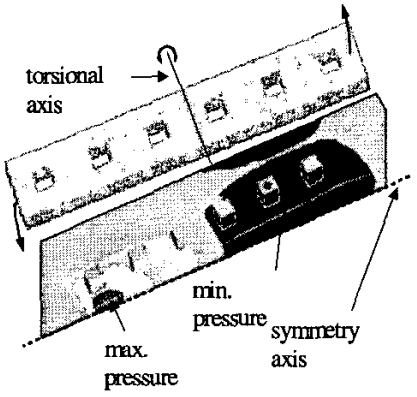

Fig. 6: Top: FEM model of a torsional test structure. Bottom: pressure distribution underneath the actuator at a left tilt.

Test structure: For the validation of the mixed-level model, we selected a simple rectangular test structure (Fig. 6) with 12 holes which is also tractable by a full FEM analysis. The dynamical device behavior calculated with the mixed level model shows a notably good agreement with NSE-based FEM simulations (Fig. 7), even for large deflections near touch down of the plate (at a tilt angle of φ=6.4°), while the computation time can be reduced from days (FEM) to minutes (mixed-level model). Combining the mixed-level damping model with compact models of the torsional springs, the mass inertia and the electric circuitry for actuation and control, we eventually arrive at a system level macromodel of the entire microsystem as displayed in Fig. 8. The compact models of the mechanical and electrical parts of the electrostatic actuator are described in [3]. Equipped with this macromodel, we are now able to study the dynamic behavior of the whole microdevice in a time-saving and cost-effective but still very accurate manner.

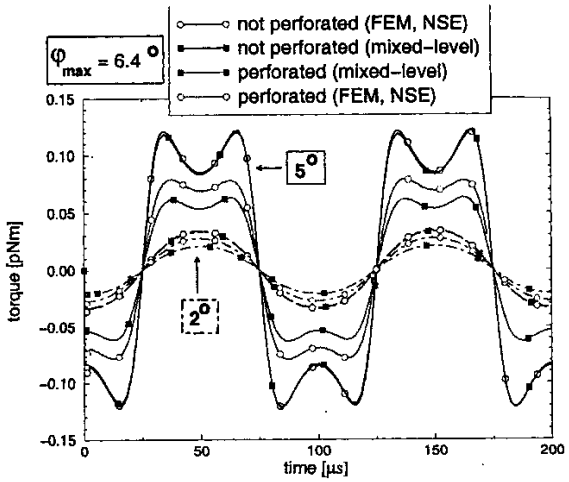

Fig. 7: Reactive torque of the actuator (Fig. 6) with and without perforation. Comparison of NSE-based results with our mixed-level model.

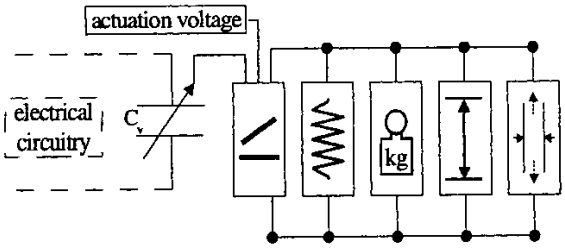

Fig. 8: System-level model of an electrostatic torsional actuator.

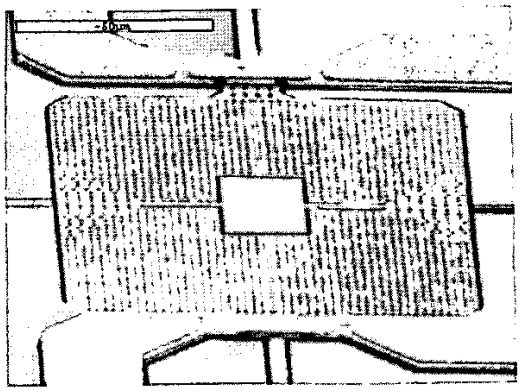

Fig. 9: SEM image of an electrostatic microswitch with about 3000 etch holes [2].

Industrial microrelay:
Much more challenging is the numerical analysis of a realistic industrial microrelay [2] with about 3000 etch holes (Fig. 9). With our model a full system analysis can be performed, but the computation time amounts to several hours. This is impracticable under industrial working conditions in a design center, and so we were motivated to derive the following method for further reduction of network nodes.

Equivalent reduced network:
The number of degrees of freedom is reduced by merging a certain set of small holes to a single hole with the same total area (Fig. 10).

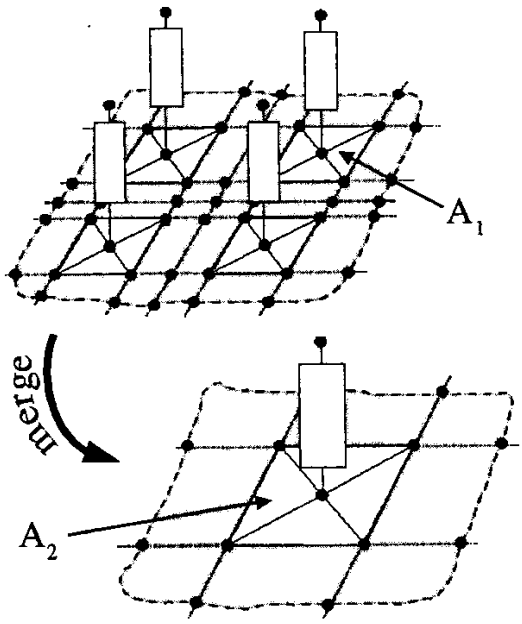

Fig. 10: Equivalent reduced network for highly perforated structures.

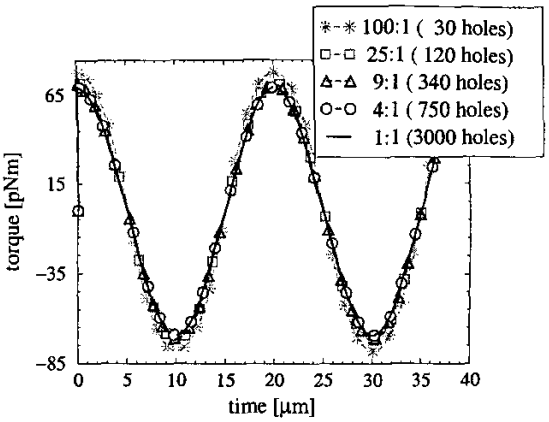

Fig. 11: Accuracy of the equivalent reduced network for various numbers of holes that have been merged.

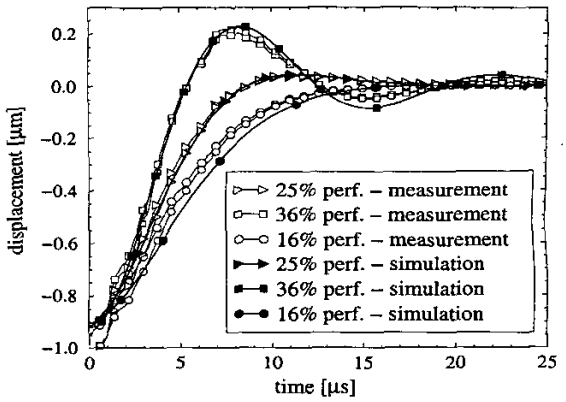

Fig. 12: Transient pull-out behavior for three different perforations of the movable electrode.

The fluidic conductance of the aperture (7) is proportional to the hole area; hence this compact model is not affected by a merging step. But the fluidic conductance of the channel (8) scales with the square of the hole area. This means that the conductance of the channel has to be scaled by the ratio of the areas (A_2/A_1) after a hole merging step.

$$Q \sim b_h^2 \sqrt{2\rho p} \qquad (7) \qquad Q \sim \frac{b_h^4 \rho}{\eta \cdot d_{plate}} \Delta p \qquad (8)$$

$$G_{aperture} \sim \text{hole area} \qquad G_{channel} \sim (\text{hole area})^2$$

It turned out that the accuracy of this approach did not significantly deteriorate with increasing node elimination, when we investigated a rectangular plate with 3000 etch holes subjected to a sinusoidal torsional motion. Fig. 11 shows that the approximation error with respect to the original model is very small – even if we merge 100 holes in one single hole.
As the computation time scales with the ratio of the merged areas, we can reduce it by two orders of magnitude.

Model validation and predictive simulation:
Finally, we compare the device behavior as predicted by the full system model with experimental data measured on industrial prototypes of a microrelay (Fig. 9). The on/off switching of three device variants with different perforation density has been measured. The perforation density reflects in the ratio of the hole area to the total cell area. Fig. 12 demonstrates the excellent agreement of our model with the real device behavior. This is the first time that the transient behavior of such a complex device could be predictively modeled on system level within a few minutes of computation time.

IV. CONCLUSIONS

We demonstrated a mixed-level model of torsional microstructures based on a physical device description in terms of a standard hardware description language (VHDL-AMS) . It makes predictive simulations possible at affordable computational expense for translational and torsional motion of highly perforated and largely deflected structures affected by air damping. As physical and geometrical quantities are input parameters of the model, it allows for fast and efficient design studies. As the model is coded in a hardware description language it can easily be linked to the electronic control circuitry of the device, so that it allows for full system simulation.

REFERENCES

[1] S. Kweon, H. Lee, H.Shin, "Modeling and Dynamic Simulation for Electrostatically Driven Micromirror", MSM 2001, pp. 334–337.
[2] R. Sattler, F. Plötz, G. Fattinger, G. Wachutka, "Modelling of an electrostatic torsional actuator: demonstrated with an RF MEMS switch", Sensors & Actuators A, Vol. 97–98C, 2002, pp. 339–348 (in press).
[3] R. Sattler, F. Plötz, S. Hoffmann, G. Wachutka, "System Level Modeling of an Electrostatic Torsional Actuator", Simulation of Semiconductor Processes and Devices 2001, Springer Verlag Wien New York, pp. 178–181.
[4] F. Pan et al., "Squeeze film damping effect on the dynamic response of a MEMS torsion mirror", J. Micromech. Microeng. 8 (1998), pp. 200–208.
[5] G. Schrag, G. Wachutka, "Physically-based Modeling of Squeeze Film Damping by Mixed-Level System Simulation, Sensors and Actuators A, Vol. 97–98C, 2002, pp.193–200 (in press) .